ZIBELINE INTERNATIONAL™ PUBLISHING

ISSN: 2521-0920 (Print)
ISSN: 2521-0602 (Online)
CODEN: MJGAAN

Malaysian Journal of Geosciences (MJG)

DOI: http://doi.org/10.26480/mjg.02.2026.64.79

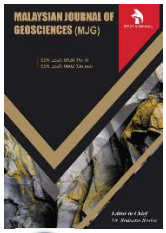

RESEARCH ARTICLE

PEBBLE MORPHOMETRIC ANALYSIS OF OLIGOCENE-MIOCENE DEPOSITS IN ASABA AND ENVIRONS, DELTA STATE, SOUTHERN NIGERIA: IMPLICATIONS FOR PALAEOENVIRONMENT AND PALAEODEPOSITION

Mba-Otike, Michael Nelson[a], Okengwu, Kingsley Onyekwere[b] and Ideozu, Richmond Uwanemesor[b]

[a] Department of Geology, Dennis Osadebay University, Asaba, Nigeria.
[b] Department of Geology University of Port Harcourt, Port Harcourt, Nigeria.
**Corresponding Author Email: mba-otike.michael@dou.edu.ng*

ARTICLE DETAILS

Article History:

Received 26 January 2026
Revised 20 February 2026
Accepted 25 February 2026
Available online 09 March 2026

ABSTRACT

This study examines Oligocene-Miocene pebbly sandstones within Asaba - Ibusa locality in southern Nigeria using the pebble morphometric analysis technique to determine the palaeoenvironmental and palaeodepositional environments. The transport history and the energy of deposition of the sediment have been inferred by examining shape, roundness, and sphericity of pebbles. Major morphometric parameters such as Zingg classification, flatness ratios, and indices of elongation were used on 237 pebble samples collected in 2 strategic sites including: Lander Brothers Quarry (Ibusa) and Dennis Osadebay University Spring (Asaba). Results indicate a fluvial dominated depositional environment, supported by high sphericity values (mean MPSI > 0.65), sub rounded pebbles (mean roundness 36–38%), and negative oblate-prolate indices (mean OPI: -1.10 to -0.61). A comparative analysis between Asaba and Ibusa pebbles indicate that there are spatial differences in palaeoflow energy and sediment transport processes with Ibusa pebbles exhibiting a little more sphericity implying a downstream rise in the energy of the fluvial. The research presents the quantitative uniqueness of the examined silt and is relevant to the idea of the processes of hinterland fluvial in the research at the time of the Oligocene-Miocene transition. These findings will enhance regional stratigraphic models and offer insights into sediment routing systems linked to Benue Trough tectonics and climatic shifts.

KEYWORDS

Pebble morphometry, fluvial environment, Niger Delta, Oligocene-Miocene, sediment transport, palaeoenvironment.

1. INTRODUCTION

The Niger Delta, one of the world's most extensively studied deltaic systems due to its hydrocarbon wealth, has seen disproportionate research focus on its marine and transitional facies of the hinterland compared to its more coastal deposits (Lawson et al., 2022; Aransiola et al., 2024). Although Oligocene-Miocene transition is an important period that affects the sediment routing systems, it has not been properly studied yet (Adeoye et al., 2022; Jolayemi et al., 2023; Ogbe et al., 2023; Omo-Irabor et al., 2024). Current literature has the disadvantage of incomplete geographic coverage, using outcrops in isolation and traditional lithostratigraphy, whereas quantitative data such as pebble morphometry; an established palaeoenvironmental reconstruction technique are not well explored. This gap is critical, as clast morphology can decode palaeoflow energy and sediment transport where other structures are poorly preserved (Anyanwu et al., 2021; Ogbe et al., 2023; Ojong et al., 2023; Kasim et al., 2023; Allen et al., 2024; Madukwe et al., 2025; Enuenwosu and Ohwo, 2024).

The aim of this study is to address these gaps in Oligocene-Miocene pebbly sandstones of two hinterland locality sites; Lander Brothers Quarry (Ibusa) and Dennis Osadebay University Spring (Asaba). Using morphometric techniques (maximum projection sphericity, oblate-prolate index, flatness-elongation ratios), we characterize depositional environments, quantify palaeoflow energy, and assess transport dynamics, with emphasis on spatial variations between sites. The Ogwashi-Asaba Formation, describing Oligocene-Miocene pebbly sandstones, lignites, and kaolinitic clays, is widely used in Niger Delta literature for this formation. Its boundary with the underlying Ameki Formation is lithologically defined by coarse, carbonaceous sandstones versus finer fossiliferous sediments.

This study makes three significant empirical contributions to understanding the Niger Delta's Oligocene-Miocene hinterland deposits. First, it provides a systematic compilation of the morphometric data of pebbly sandstones of this area, giving the baseline values of the sphericity, oblate-prolate index, and the flatness-elongation ratios that were not previously available. Second, the comparative analysis of Ibusa and Asaba sites demonstrates that there were significant spatial differences in the energy of palaeoflow and sediment transport processes of the ancient fluvial system. Third, it provides crucial foundational data that will enable future studies to correlate hinterland fluvial facies with delta-front reservoirs, support potential ICS-compliant formalization of the Ogwashi-Asaba Formation through proposed type sections, and contribute to more integrated tectono-sedimentary models linking Benue Trough dynamics to deltaic progradation patterns.

Quick Response Code	Access this article online	
	Website: www.myjgeosc.com	**DOI:** 10.26480/mjg .02.2026.64.79

Cite the Article: Mba-Otike, Michael Nelson, Okengwu, Kingsley Onyekwere and Ideozu, Richmond Uwanemesor (2026). Pebble Morphometric Analysis of Oligocene-Miocene Deposits in Asaba and Environs, Delta State, Southern Nigeria: Implications for Palaeoenvironment and Palaeodeposition. Malaysian Journal of Geosciences, 10(2): 64-79.

1.1 Geological Setting and Study Area

The Niger Delta Basin emerged as a major regressive depocenter following the South Atlantic Ocean's opening during the Late Jurassic to Early Cretaceous (Chima et al., 2022; Zhang et al., 2023; Eze et al., 2024; Adijoh et al., 2025). A component of the West African rift system that was related to the separation of the African-South American plates, the delta proper began concurrently with the Paleocene (around 60 Ma) and has been slowly prograding since that point over a distance of 300 km into the Gulf of Guinea, developing over 12 km of sediments in the central depozones (Tijani, 2023; Odesa et al., 2024; Yuan et al., 2025; Ajidahun et al., 2025; Wali et al., 2021 and Alamu, 2023)

The stratigraphy of the delta is based on the usual tri-partite separation, with three diachronous formations that are basinward-younging (Table 1). The Deep-sea marine shales that make up the basal Akata Formation form the origin of the hydrocarbons as well as the surface on which growth faults detach (Ideozu et al., 2025a, b, c). Overlying this, the Agbada Formation's alternating sands and shales represent delta-front to shoreface environments, hosting the delta's major reservoirs through coarsening-upward parasequences (Mba-Otike et al., 2025). The topmost Benin Formation consists of the massive sands of the fluvial and upper delta plain which get thickened in the landward direction (Udo et al., 2023).

Table 1: Stratigraphic framework of the Niger Delta showing formation names, lithologies, and ages, (modified from (Mba-Otike et al., 2025a, b, c; Ideozu et al., 2025).

SUBSURFACE			SURFACE OUTCROPS		
YOUNGEST KNOWN AGE	**FORMATION**	**OLDEST KNOWN AGE**	**YOUNGEST KNOWN AGE**	**FORMATION**	**OLDEST KNOWN AGE**
Recent	Benin Formation	Oligocene	Pleistocene	Benin Formation	Oligocene
Pliocene	Agbada Formation	Eocene	Miocene	Ogwashi-Asaba Formation??	Oligocene
			Middle Eocene	Ameki Formation	Early Eocene
Miocene	Akata Formation	Palaeocene	Early Eocene	Imo Formation	Late Cretaceous

The Oligocene-Miocene interval represents a pivotal phase marked by extensive fluvial progradation across the northern delta plain (Ojenabor et al., 2024). This period saw: (1) establishment of permanent drainage networks linking the Benue Trough (Salim, 2021), (2) increased sediment flux from Cameroon Volcanic Line uplift and basement reactivation, and (3) climate-driven shifts in weathering regimes (Chima et al., 2022; Tijani, 2023; Amasi et al., 2021; Adijoh et al., 2023; Samal et al., 2023). Provenance studies reveal mixed contributions from Precambrian Basement Complex rocks, Cretaceous Benue Trough sediments, and recycled deltaic deposits, with sediment routing primarily controlled by the Anambra Basin conduit and secondary inputs from the Cameroon Volcanic Line (Ejeh, 2021; Oyebanjo et al., 2021; Omoruyi et al., 2022; Ndjigui et al., 2023; Anyiam et al., 2021; Sun et al., 2022).

This study concentrates on the Ibusa-Asaba axis (Figure 2) which is a 19 km NE-SW trending axis of Delta state that exposes Oligocene-Miocene hinterland deposits. Two strategic locations; Ibusa (6°11'N, 6°38'E) and Asaba (6°12'N, 6°44'E) bore pebbles, providing critical insights into how hinterland processes shaped the delta's evolution during this key progradational phase.

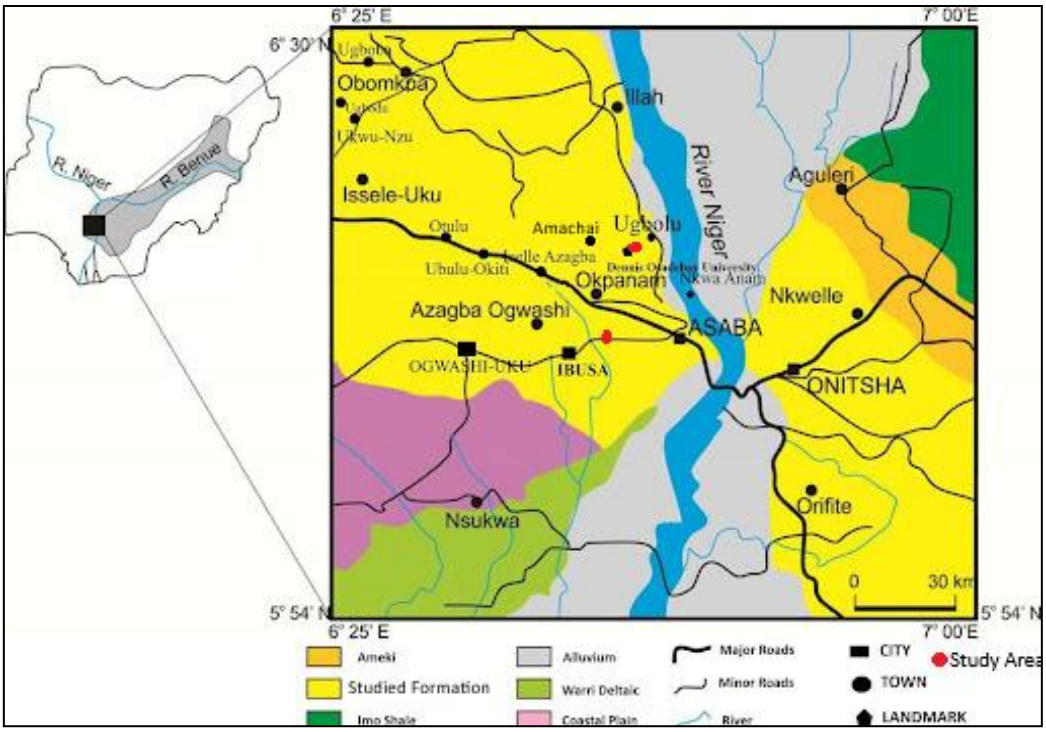

Figure 1: Geologic map of the study area showing sample locations (Lander Brothers Quarry and Dennis Osadebay University Spring) in red.

2. METHODOLOGY

Comprehensive pebble morphometric analysis of the Oligocene-Miocene pebbly-sandstones revealed in the Ibusa-Asaba axis was used in this study, which combined field sampling and quantitative laboratory analysis to provide an explanation of the depositional settings. The total number of intact pebbles was 237 and was distributed in an organized manner and through randomized stratified sampling technique across the two sites of study in order to gain a representative coverage of the fluvial depositional system, whilst avoiding sampling bias of broken or weathered pebbles. The length of each pebble (L), intermediate (I), and short (S) axis (Figure 2a) underwent specific dimensional measurements with the help of digital calipers at the accuracy of 0.1 mm according to the established sedimentological procedures (Sneed and Folk, 1958; Dobkins and Folk, 1970). These measurements were used to compute major morphometric indices as presented in Table 2.

Table 2: Key morphometric formulae applied in pebble analysis, including: 1) Maximum Projection Sphericity Index (MPSI), 2) Oblate-Prolate Index (OPI), and 3) Wadell's roundness, following methodologies from (Ideozu and Ikoro, 2015; Okon et al., 2018; Okon and Ojong, 2019)

S/N	Formula	Reference
1	Maximum Projection Sphericity Index (MPSI) = $\{S^2/LI\}^{1/3}$	Sneed and Folk (1958)
2	Elongation Ratio (ER) = I/L	Lutig (1962), Sames (1966)
3	Flatness Ratio FR = S/L	Lutig (1962)
4	Flatness Index = (L – I + S) / L	Illenberger (1991)
5	Oblate – Prolate Index, OPI = $10((L-I)/(L-S)-(0.50)]/S/L$	Dobkins and Folk (1970)
6	Roundness $[(\sum r)/nR]$	Wadell (1932)

The analytical regional framework integrated several methods of interpreting the depositional environment, which started with bivariate plots of MPSI or OPI and Flatness or Sphericity with known environmental limits used to identify fluvial or other depositional environments. Another key point of the analysis was the use of the roundness index described (Figure 2b) which gave quantitative evaluation of the surface curvature of pebbles, by means of meticulous measurement of the proportion of convexity of the maximum projection perimeters by (Wadell, 1932). This was a very rigorous method of evaluating roundness that is more time-consuming than the visual techniques of evaluation, but it was much more accurate in determining the history of abrasion and the energy of transport of the particles (Pissart et al., 1998; Roussillon et al., 2009).

The morphmetric data set was statistically analyzed using the Wadell-derived roundness values as well as other parameters (including the ones that are used to classify the pebbles into categories according to their form and shape - Table 3) with the mean values and SDs being calculated to make the comparison between Ibusa and Asaba sites robust. Such quantitative data, such as the detailed roundness data, were combined with the observation of the qualitative sedimentology and lithological characteristics in the context of established sedimentological frameworks and compared with other similar systems gave further background to the interpretation of the environment (Bluck, 1967; Stratten, 1974; Okoro et al., 2012). The approachology had stringent quality control measures of all parameters, and emphasis was made in the roundness measurements of Wadell, by using standardized protocols, calibrated instruments, and repeated measurements to ascertain consistency in data.

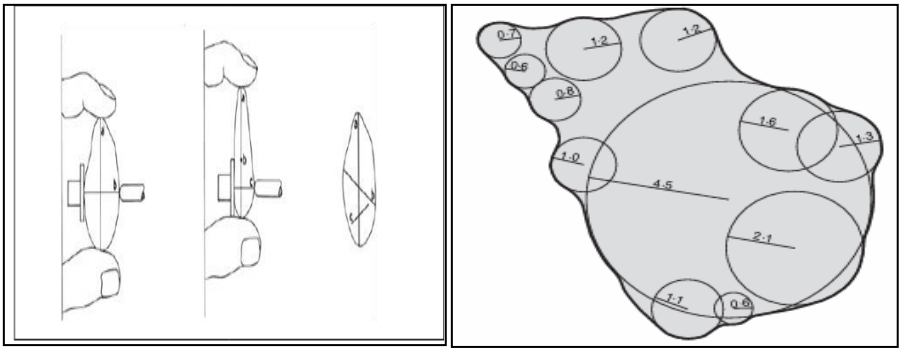

Figure 2: (a) Measurement protocol for pebble morphometric analysis (from Madi and Ndlazi (2020)) (b) Methodology for particle roundness measurement (after Wadell, 1932)

Table 3: Classification thresholds for pebble forms based on axial ratios (I/L and S/I), showing Zingg-type categories including: Compact (C), Compact Elongate (CE), Compact Bladed (CB), Compact Prolate (CP), Elongate (E), Bladed (B), Prolate (P), Very Bladed (VB), and Very Elongate (VE). Modified from (Dobkins and Folk, 1970; Omosanya and Alves, 2013).

Category	I/L	S/I	Interpretation
C (Compact)	≥ 0.67	≥ 0.67	Nearly equant (compact)
CE (Compact Elongate)	≥ 0.67	0.5 – 0.67	Almost compact, slightly flat
CB (Compact Bladed)	0.5 – 0.67	≥ 0.67	Nearly compact but bladed
CP (Compact Prolate)	≥ 0.67	≤ 0.5	Compact but elongated
E (Elongate)	≥ 0.67	< 0.67	Longer than wide
B (Bladed)	< 0.67	≥ 0.67	Thin, flat shape
P (Prolate)	≥ 0.67	< 0.5	Rod-like shape
VB (Very Bladed)	< 0.5	≥ 0.67	Extremely flat and wide
VE (Very Elongate)	≥ 0.75	< 0.5	Extremely rod-like

The reliability of the interpretations was improved by cross-validation with the known environmental thresholds such as the ones related to roundness in the various depositional environments. Such a combined method, incorporating the accurate analysis of roundness by Wadell and other morphometric and sedimentological data, provided the possibility to construct in detail the palaeoflow conditions, the history of the sediment transportation, and the energy regimes of the depositional environment. The roundness data was particularly useful in identifying the fluvial sub-environments in addition to determining the post-depositional modification processes in the pebbly sandstones of interest in this study. The quantitative roundness evaluation of Wadell when combined with other morphometric studies and classical sedimentological studies presented a very strong method of interpreting the depositional history of such Oligocene-Miocene hinterland deposits in the Niger Delta

basin.

Bivariate plots were used to cause distinction between fluvial and beach environments by the use of morphmetric data: MPSI vs. OPI plots and were determined by using the known environmental thresholds (Dobkins and Folk, 1970): MPSI = 0.65 and OPI = -1.5 are commonly used as political indications. Flatness vs. Sphericity plots also served as an extra discrimination measure in that fluvial pebbles tended to be more spheric and intermediate in flatness than were beach pebbles. All morphometric parameters were calculated using statistical analysis, which involved the determination of mean values and the standard deviation of all morphometric parameters to compare the two sites of Ibusa and Asaba. The combination of morphometric and lithological data was a robust foundation of the interpretation of the palaeoflow conditions, history of the sediment transportation, and deposition environment of studied pebbly sandstones.

3. Results and Discussion

The exposure at Location 1 (06°16'03.1''N, 006°42'12''E) is situated at a perennial spring within the Dennis Osadebay University, Asaba premises, and it exhibits a well-defined 19.6-foot (5.97 meters) thick section of the Oligocene-Miocene sediments. This exposure displays a fining-downward lithologic sequence, divided into three main sedimentary units, each recording distinct depositional environments and processes. Notably,

Figure 3a, and Figure 3b give graphic record of these stratigraphic intervals, Figure 3a showing the bottom unit of clay, the overlapping layer of clay sands and the spring point at their intersection, and Figure 3b showing the uppermost pebbly sandstone layer. The spring allows a hydrogeological contact between the clay and the sandstone units; an impermeable lithologic boundary that causes groundwater to reach the surface because of the impermeability of the underlying clays.

Outcrop has three lithologic units. Below, grey, clay is found between 0 and 1.13 meters of age, is of low-energy floodplain deposition with reducing conditions, and is an aquitard related to spring emergence. Over this, to 4.30 meters deep, clayey sands are deposited, in what may be considered a moderately active fluvial environment with evidence of bioturbation and oxidation, which indicate a levee or crevasse splay. The upper layer, 5.97 meters, is indistinct, ill-sorted pebbly sandstone which denotes high energy channel deposition. This sandstone was sampled (L1) to analyse the morphometric and petrographic properties of pebbles, which will help to understand the provenance and the processes of its deposition.

A combination of the lithological and sedimentological characteristics observed at Location 1 and old testifies to deposition in a high-energy fluvial environment, with a background of low-energy clays of the floodplain being replaced by higher-energy sandy and pebbly channel loads. The statement of vertical facies variation coupled with hydrogeological structures including the spring support the explanations of a dynamic fluvio-deltaic depositional system characteristic of Oligocene-Miocene Sediments.

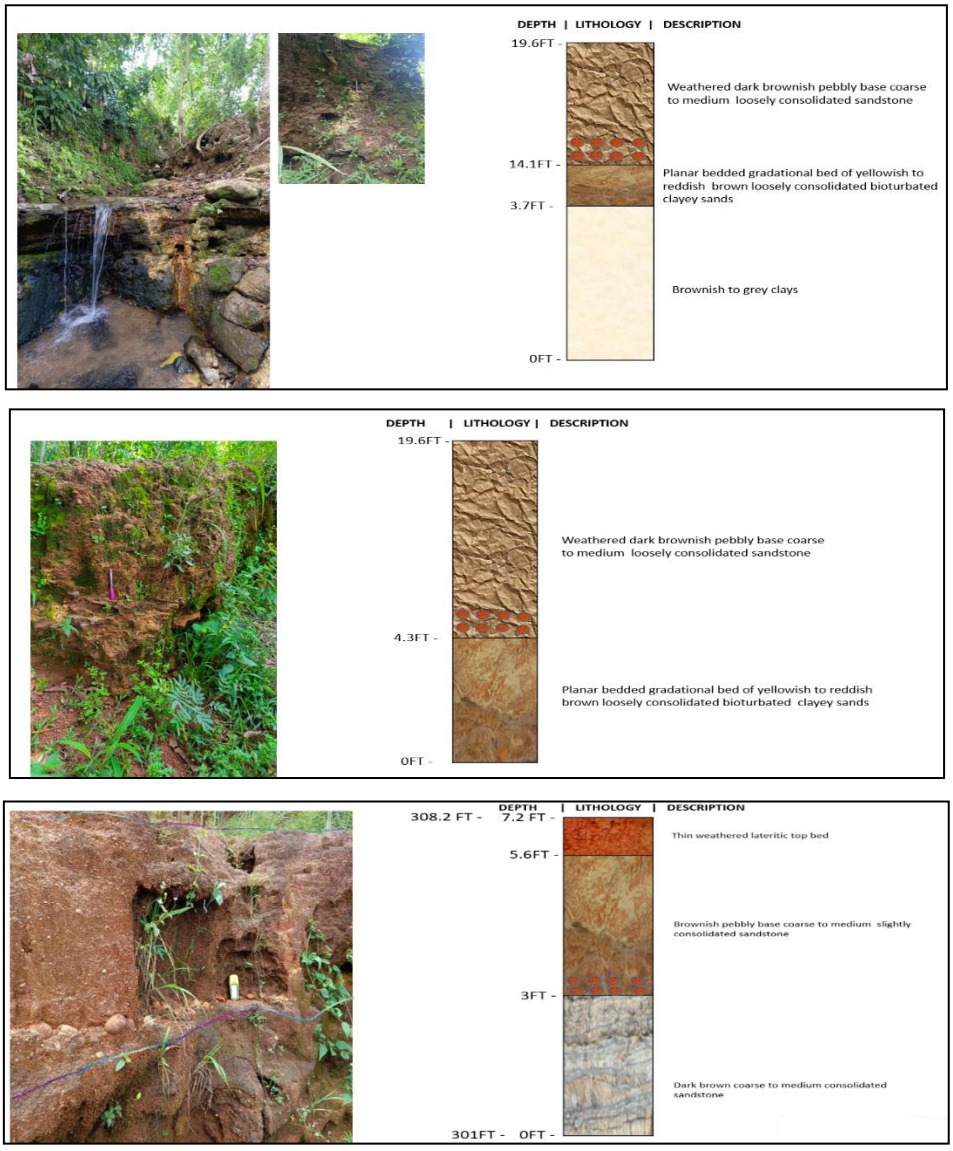

Figure 3a: (1) Field photograph and (2) stratigraphic log of Location 1a (Dennis Osadebay University Spring, Asaba) showing: (i) brownish to gray clays (0 – 3.7 ft), (ii) yellowish to reddish brown clayey sands (3.7– 14.1 ft) and (iii) weathered pebbly base loosely consolidated sandstones

Figure 3b: (1) Field photograph and (2) stratigraphic log of Location 1b (Dennis Osadebay University Spring, Asaba) showing: (i) yellowish to reddish clayey sands (0–4.3 ft) and (ii) pebbly base loosely consolidated sandstones (4.3–19.6 ft).

Figure 3c: (1) Field photograph and (2) detailed litholog of Location 2 (Active Lander Sandstone Quarry, Ibusa) showing: (i) 3 ft basal consolidated sandstone, (ii) 2.6 ft pebbly sandstone unit, and (iii) capping lateritic layer. Sample L2 was collected from the pebbly sandstone interval.

Location 2 can be seen at the lander brothers quarry, Ibusa (N06°11' 19.9" and E006°39' 33.6"). This part of the outcrop is a relatively shorter exposure of 7.2 feet with a starting point of 301 feet in height (Figure 3c). It has a dark brown, rough-to-median-grained consolidated sandstone at the base, and then 2.6 feet of brownish pebbly sandstone. The sequence has a thin layer of laterite at the top and ends at 308.2 feet. Interestingly, samples of pebbles (Sample L2) to be used in morphmetric and petrographic analysis were also taken in this area, especially in the unit of pebbly sandstones.

Collectively, these parts provide a record of a very changeable depositional environment, which brings out the interaction of a combination of fluvial and deltaic processes with intermittent exposure and weathering. The facies differences both laterally and vertically indicate changes in depositional energy, sediment supply and palaeohydrological processes in this section of the Oligocene-Miocene Sediments which are being seen in this region.

The Table 4 and Table 5 provide the spreadsheet of the measured values and some calculations of the pebbles. When pebble form is analyzed by the use of the Sneed and Folk (1958) diagram of Asaba sample, it is found that the compact-bladed form occupies 55 percent, compact platy form occupies 39 percent and only 6 percent of the samples are occupied by compact in terms of form. The mean lengths of the axes of the pebbles are 34 mm in long axis, 30 mm in intermediate axis and 26 mm in short axis. In the case of the Ibusa pebbles, the Sneed and Folk (1958) graph also shows that the compact platy shape occupies 51% of the number, the compact-bladed shape occupies 46% of the number and only 3 percent of the number is compact. These pebbles had an average axis of 40 mm (long axis), 35mm (intermediate axis) and 30mm (short axis).

Table 4: Summary of Data from pebble morphometric analysis and calculations for Asaba Pebbles

Location 1 Dennis Osadebay University Spring - Asaba												
S/N	L	S	I	I/L	S/I	S/L	S^2	OPI	FI	ROUNDNESS	MPSI	FI
1	1.87	1.63	1.74	0.93	0.94	0.87	2.66	0.48	1.57	0.31	2.72	87.17
2	2.15	1.55	1.88	0.87	0.82	0.72	2.40	-0.69	1.98	0.31	1.98	72.09
3	1.99	1.69	1.86	0.93	0.91	0.85	2.86	-0.79	1.50	0.33	2.57	84.92
4	2.31	1.94	2.28	0.99	0.85	0.84	3.76	-4.99	0.97	0.34	2.38	83.98
5	2.4	2.29	2.38	0.99	0.96	0.95	5.24	-3.33	1.04	0.35	3.06	95.42
6	2.57	1.37	2.21	0.86	0.62	0.53	1.88	-3.75	1.93	0.36	1.10	53.31
7	2.69	1.57	2.2	0.82	0.71	0.58	2.46	-1.07	2.41	0.37	1.39	58.36
8	2.28	1.88	2.29	1	0.82	0.82	3.53	-6.37	0.78	0.38	2.26	82.46
9	2.65	1.48	2.42	0.91	0.61	0.56	2.19	-5.43	1.43	0.39	1.14	55.85
10	2.26	1.57	2.07	0.92	0.76	0.69	2.46	-3.23	1.54	0.40	1.76	69.47
11	2.49	2.01	2.35	0.94	0.86	0.81	4.04	-2.58	1.37	0.41	2.30	80.72
12	3.1	2.03	2.8	0.9	0.73	0.65	4.12	-3.35	1.62	0.42	1.58	65.48
13	2.41	2.29	2.33	0.97	0.98	0.95	5.24	1.75	1.28	0.43	3.11	95.02
14	3.1	1.37	2.57	0.83	0.53	0.44	1.88	-4.38	2.15	0.44	0.79	44.19
15	4.85	3.27	4.2	0.87	0.78	0.67	10.69	-1.31	2.01	0.31	1.75	67.42
16	3.58	2.39	3.07	0.86	0.78	0.67	5.71	-1.07	2.09	0.45	1.73	66.76
17	3.3	2.37	3.01	0.91	0.79	0.72	5.62	-2.62	1.60	0.32	1.88	71.82
18	2.61	2.11	2.55	0.98	0.83	0.81	4.45	-4.70	1.04	0.33	2.23	80.84
19	3.21	2.73	3.01	0.94	0.91	0.85	7.45	-0.98	1.47	0.34	2.57	85.05
20	2.46	1.88	2.39	0.97	0.79	0.76	3.53	-4.96	1.05	0.35	2.00	76.42
21	3.03	1.86	2.59	0.85	0.72	0.61	3.46	-2.02	2.07	0.35	1.47	61.39
22	3.8	2.73	3.33	0.88	0.82	0.72	7.45	-0.85	1.96	0.36	1.96	71.84
23	2.85	2.44	2.71	0.95	0.9	0.86	5.95	-1.85	1.35	0.37	2.57	85.61
24	3.16	2.52	2.88	0.91	0.88	0.80	6.35	-0.78	1.68	0.38	2.33	79.75
25	5.34	4.14	4.83	0.9	0.86	0.78	17.14	-0.97	1.73	0.39	2.22	77.53
26	3.93	3.11	3.5	0.89	0.89	0.79	9.67	0.31	1.89	0.40	2.34	79.13
27	3.12	2.58	2.89	0.93	0.89	0.83	6.66	-0.90	1.56	0.41	2.46	82.69
28	3.31	2.58	3.04	0.92	0.85	0.78	6.66	-1.67	1.60	0.42	2.21	77.95
29	2.86	1.99	2.56	0.9	0.78	0.70	3.96	-2.23	1.74	0.43	1.80	69.58
30	2.72	1.91	2.33	0.86	0.82	0.70	3.65	-0.26	2.14	0.44	1.92	70.22
31	3.14	2.63	3.04	0.97	0.87	0.84	6.92	-3.63	1.16	0.31	2.42	83.76

Table 4(cont): Summary of Data from pebble morphometric analysis and calculations for Asaba Pebbles												
32	4.48	3.47	3.69	0.82	0.94	0.77	12.04	3.64	2.54	0.32	2.43	77.46
33	6.2	3.76	4.24	0.68	0.89	0.61	14.14	5.00	3.77	0.33	1.79	60.65
34	3.6	3.15	3.43	0.95	0.92	0.88	9.92	-1.40	1.35	0.33	2.68	87.50
35	3.62	2.55	3.11	0.86	0.82	0.70	6.50	-0.33	2.11	0.35	1.93	70.44
36	3.95	3.43	3.9	0.99	0.88	0.87	11.76	-4.65	0.99	0.36	2.55	86.84
37	2.34	2.15	2.33	1	0.92	0.92	4.62	-4.87	0.96	0.36	2.83	91.88
38	2.93	1.99	2.56	0.87	0.78	0.68	3.96	-1.57	1.94	0.37	1.76	67.92
39	3.48	2.86	3.21	0.92	0.89	0.82	8.18	-0.79	1.60	0.38	2.44	82.18
40	2.61	2.03	2.38	0.91	0.85	0.78	4.12	-1.33	1.66	0.39	2.21	77.78
41	2.59	1.89	2.38	0.92	0.79	0.73	3.5721	-2.741	1.54	0.40	1.93	72.97
42	2.1	1.9	1.98	0.94	0.96	0.90	3.61	1.1053	1.48	0.41	2.89	90.48
43	2.8	2.72	2.75	0.98	0.99	0.97	7.3984	1.2868	1.15	0.42	3.20	97.14
44	3.16	2.46	2.87	0.91	0.86	0.78	6.0516	-1.101	1.7	0.44	2.22	77.85
45	4.16	3.68	3.79	0.91	0.97	0.88	13.542	3.0616	1.77	0.48	2.86	88.46
46	5.21	3.72	4.59	0.88	0.81	0.71	13.838	-1.175	1.9	0.31	1.93	71.40
47	4.03	3.44	3.67	0.91	0.94	0.85	11.834	1.2906	1.75	0.32	2.67	85.36
48	4.53	3.39	4.12	0.91	0.82	0.75	11.492	-1.875	1.65	0.33	2.05	74.83
49	3.43	3.02	3.2	0.93	0.94	0.88	9.1204	0.6925	1.55	0.34	2.77	88.05
50	5.64	4.36	5.05	0.9	0.86	0.77	19.01	-0.505	1.82	0.35	2.22	77.30
51	5	3.96	4.07	0.81	0.97	0.79	15.682	4.9777	2.65	0.36	2.57	79.20
52	4.01	2.79	3.43	0.86	0.81	0.70	7.7841	-0.353	2.14	0.38	1.89	69.58
53	5.81	4.46	5.3	0.91	0.84	0.77	19.892	-1.592	1.65	0.39	2.15	76.76
54	4.26	3.34	3.78	0.89	0.88	0.78	11.156	0.2773	1.91	0.40	2.31	78.40
55	5.47	3.65	4.47	0.82	0.82	0.67	13.323	0.7411	2.5	0.40	1.82	66.73
56	3.68	3.1	3.4	0.92	0.91	0.84	9.61	-0.205	1.6	0.41	2.56	84.24
57	4.6	3.08	3.92	0.85	0.79	0.67	9.4864	-0.786	2.15	0.43	1.75	66.96
58	4.18	3.7	3.84	0.92	0.96	0.89	13.69	2.3536	1.7	0.43	2.84	88.52
59	3.33	3.09	3.12	0.94	0.99	0.93	9.5481	4.0413	1.56	0.44	3.06	92.79
MEAN	3.44	2.63	3.08	0.91	0.85	0.77	7.54	-1.10	1.71	0.38	2.21	77.05
SD	1.05	0.80	0.84	0.06	0.09	0.11	4.52	2.49	0.49	0.04	0.51	10.93

L - Long Axis, S - Short Axis, I - Intermediate Axis, I/L - Elongation Ratio (ER), S/L - Flatness Ratio (FR), S/I - Another measure of flatness, OPI - Oblate – Prolate (OP) Index, MPSI - Maximum Projection Sphericity Index, FI - Flatness Index.

Table 5: Summary of Data from pebble morphometric analysis and calculations for Ibusa Pebbles													
Location 2 Lander Brother Quarry - Ibusa													
S/N	L	S	I	I/L	S/I	S/L	L-I	L-S	S2	OPI	LI	MPSI	FI
1	5.68	3.67	4.76	0.84	0.77	0.65	0.92	2.01	13.47	-0.65	27.04	1.66	0.31
2	5.83	2.99	4.1	0.70	0.73	0.51	1.73	2.84	8.94	2.13	23.90	1.25	0.39
3	4.55	3.83	4.25	0.93	0.90	0.84	0.3	0.72	14.67	-0.99	19.34	2.53	0.33
4	4.49	4.08	4.29	0.96	0.95	0.91	0.2	0.41	16.65	-0.13	19.26	2.88	0.40
5	4.14	3.59	4.29	1.04	0.84	0.87	-0.2	0.55	12.89	-8.91	17.76	2.42	0.35
6	3.24	2.84	3.09	0.95	0.92	0.88	0.15	0.4	8.07	-1.43	10.01	2.69	0.42
7	4.18	3.66	4.06	0.97	0.90	0.88	0.12	0.52	13.40	-3.07	16.97	2.63	0.34

Table 5 (cont): Summary of Data from pebble morphometric analysis and calculations for Ibusa Pebbles

8	4.07	3.23	3.81	0.94	0.85	0.79	0.26	0.84	10.43	-2.40	15.51	2.24	0.37
9	5.96	4.11	5.57	0.93	0.74	0.69	0.39	1.85	16.89	-4.19	33.20	1.70	0.40
10	5.03	3.68	4.57	0.91	0.81	0.73	0.46	1.35	13.54	-2.18	22.99	1.96	0.34
11	3.89	2.65	3.07	0.79	0.86	0.68	0.82	1.24	7.02	2.37	11.94	1.96	0.43
12	4.01	3.29	3.6	0.90	0.91	0.82	0.41	0.72	10.82	0.85	14.44	2.50	0.36
13	4.5	2.68	3.41	0.76	0.79	0.60	1.09	1.82	7.18	1.66	15.35	1.56	0.41
14	5.22	3.68	4.74	0.91	0.78	0.70	0.48	1.54	13.54	-2.67	24.74	1.82	0.38
15	4.47	2.72	3.73	0.83	0.73	0.61	0.74	1.75	7.40	-1.27	16.67	1.48	0.32
16	4.36	3.45	4.05	0.93	0.85	0.79	0.31	0.91	11.93	-1.99	17.66	2.25	0.45
17	5.94	4.74	5.09	0.86	0.93	0.80	0.85	1.2	22.47	2.61	30.23	2.48	0.36
18	5.81	5.27	5.67	0.98	0.93	0.91	0.14	0.54	27.77	-2.65	32.94	2.81	0.43
19	6.07	5.69	5.87	0.97	0.97	0.94	0.2	0.38	32.38	0.28	35.63	3.03	0.37
20	5.56	4.96	5.44	0.98	0.91	0.89	0.12	0.6	24.60	-3.36	30.25	2.71	0.39
21	7.45	5.92	6.62	0.89	0.89	0.79	0.83	1.53	35.05	0.53	49.32	2.37	0.30
22	6.69	5.86	6.47	0.97	0.91	0.88	0.22	0.83	34.34	-2.68	43.28	2.64	0.42
23	7.34	5.08	6.67	0.91	0.76	0.69	0.67	2.26	25.81	-2.94	48.96	1.76	0.35
24	7.16	5.66	6.36	0.89	0.89	0.79	0.8	1.5	32.04	0.42	45.54	2.34	0.38
25	6.77	4.76	6.29	0.93	0.76	0.70	0.48	2.01	22.66	-3.71	42.58	1.77	0.44
26	5.79	4.58	5.61	0.97	0.82	0.79	0.18	1.21	20.98	-4.44	32.48	2.15	0.31
27	5.74	4.71	4.76	0.83	0.99	0.82	0.98	1.03	22.18	5.50	27.32	2.71	0.40
28	4.36	3.82	4.09	0.94	0.93	0.88	0.27	0.54	14.59	0.00	17.83	2.73	0.36
29	3.51	2.39	2.68	0.76	0.89	0.68	0.83	1.12	5.71	3.54	9.41	2.02	0.42
30	3.35	2.68	3.05	0.91	0.88	0.80	0.3	0.67	7.18	-0.65	10.22	2.34	0.38
31	3.86	2.84	3.6	0.93	0.79	0.74	0.26	1.02	8.07	-3.33	13.90	1.93	0.41
32	3.42	2.38	2.99	0.87	0.80	0.70	0.43	1.04	5.66	-1.24	10.23	1.85	0.33
33	3.51	2.56	3.02	0.86	0.85	0.73	0.49	0.95	6.55	0.22	10.60	2.06	0.44
34	3.12	2.74	2.96	0.95	0.93	0.88	0.16	0.38	7.51	-0.90	9.24	2.71	0.36
35	3.89	2.79	3.26	0.84	0.86	0.72	0.63	1.1	7.78	1.01	12.68	2.05	0.43
36	3.57	2.75	3	0.84	0.92	0.77	0.57	0.82	7.56	2.53	10.71	2.35	0.37
37	4.37	3.57	4.23	0.97	0.84	0.82	0.14	0.8	12.74	-3.98	18.49	2.30	0.41
38	4.18	3.69	3.7	0.89	1.00	0.88	0.48	0.49	13.62	5.43	15.47	2.93	0.34
39	3.59	3	3.3	0.92	0.91	0.84	0.29	0.59	9.00	-0.10	11.85	2.53	0.39
40	2.76	2.56	2.59	0.94	0.99	0.93	0.17	0.2	6.55	3.77	7.15	3.06	0.33
41	3.34	2.75	2.89	0.87	0.95	0.82	0.45	0.59	7.56	3.19	9.65	2.61	0.44
42	3.03	2.58	2.73	0.90	0.95	0.85	0.3	0.45	6.66	1.96	8.27	2.68	0.36
43	3.14	2.44	2.67	0.85	0.91	0.78	0.47	0.7	5.95	2.21	8.38	2.37	0.40
44	2.95	1.55	2.49	0.84	0.62	0.53	0.46	1.4	2.40	-3.26	7.35	1.09	0.37
45	2.67	2.34	2.16	0.81	1.08	0.88	0.51	0.33	5.48	11.93	5.77	3.16	0.42
46	3.93	1.83	3.22	0.82	0.57	0.47	0.71	2.1	3.35	-3.48	12.65	0.88	0.33
47	2.57	2.26	2.49	0.97	0.91	0.88	0.08	0.31	5.11	-2.75	6.40	2.66	0.39
48	4.37	3.77	3.67	0.84	1.03	0.86	0.7	0.6	14.21	7.73	16.04	2.95	0.45

Table 5 (cont): Summary of Data from pebble morphometric analysis and calculations for Ibusa Pebbles

49	3.01	2.27	2.53	0.84	0.90	0.75	0.48	0.74	5.15	1.97	7.62	2.26	0.32
50	2.73	2.43	2.63	0.96	0.92	0.89	0.1	0.3	5.90	-1.87	7.18	2.74	0.40
51	28.9	2.15	2.57	0.09	0.84	0.07	26.3	26.8	4.62	65.10	74.27	0.21	0.37
52	3.1	2.77	3.03	0.98	0.91	0.89	0.07	0.33	7.67	-3.22	9.39	2.72	0.43
53	2.65	1.73	2.6	0.98	0.67	0.65	0.05	0.92	2.99	-6.83	6.89	1.45	0.35
54	2.84	1.8	2.3	0.81	0.78	0.63	0.54	1.04	3.24	0.30	6.53	1.65	0.41
55	3.08	2.59	2.92	0.95	0.89	0.84	0.16	0.49	6.71	-2.06	8.99	2.49	0.38
56	2.21	1.55	1.96	0.89	0.79	0.70	0.25	0.66	2.40	-1.73	4.33	1.85	0.42
57	2.63	2.03	2.33	0.89	0.87	0.77	0.3	0.6	4.12	0.00	6.13	2.24	0.34
58	2.31	2.11	2.14	0.93	0.99	0.91	0.17	0.2	4.45	3.83	4.94	3.00	0.41
59	2.44	2.09	2.31	0.95	0.90	0.86	0.13	0.35	4.37	-1.50	5.64	2.58	0.37
60	3.03	1.95	2.45	0.81	0.80	0.64	0.58	1.08	3.80	0.58	7.42	1.71	0.44
61	2.7	2.07	2.21	0.82	0.94	0.77	0.49	0.63	4.28	3.62	5.97	2.39	0.32
62	2.73	1.9	2.26	0.83	0.84	0.70	0.47	0.83	3.61	0.95	6.17	1.95	0.39
63	5.73	3.27	4.71	0.82	0.69	0.57	1.02	2.46	10.69	-1.50	26.99	1.32	0.35
64	4.7	4.02	4.35	0.93	0.92	0.86	0.35	0.68	16.16	0.17	20.45	2.63	0.43
65	4.12	3.62	4.08	0.99	0.89	0.88	0.04	0.5	13.10	-4.78	16.81	2.60	0.37
66	3.54	3.04	3.56	1.01	0.85	0.86	-0	0.5	9.24	-6.29	12.60	2.44	0.41
67	3.65	2.92	3.15	0.86	0.93	0.80	0.5	0.73	8.53	2.31	11.50	2.47	0.35
68	5.83	4.11	5.26	0.90	0.78	0.70	0.57	1.72	16.89	-2.39	30.67	1.84	0.44
69	4.46	3.79	4.34	0.97	0.87	0.85	0.12	0.67	14.36	-3.78	19.36	2.47	0.36
70	4.86	2.94	4.04	0.83	0.73	0.60	0.82	1.92	8.64	-1.21	19.63	1.47	0.40
71	4.65	2.79	4.21	0.91	0.66	0.60	0.44	1.86	7.78	-4.39	19.58	1.33	0.38
72	3.47	3.44	3.45	0.99	1.00	0.99	0.02	0.03	11.83	1.68	11.97	3.29	0.43
73	3.65	2.04	3.21	0.88	0.64	0.56	0.44	1.61	4.16	-4.06	11.72	1.18	0.34
74	4.69	3.57	4.09	0.87	0.87	0.76	0.6	1.12	12.74	0.47	19.18	2.21	0.40
75	4.48	2.17	3.98	0.89	0.55	0.48	0.5	2.31	4.71	-5.85	17.83	0.88	0.36
76	3.78	2.98	3.08	0.81	0.97	0.79	0.7	0.8	8.88	4.76	11.64	2.54	0.42
77	3.66	1.94	3.11	0.85	0.62	0.53	0.55	1.72	3.76	-3.40	11.38	1.10	0.35
78	3.87	3.71	3.73	0.96	0.99	0.96	0.14	0.16	13.76	3.91	14.44	3.18	0.41
79	6.95	5.16	5.79	0.83	0.89	0.74	1.16	1.79	26.63	1.99	40.24	2.21	0.38
80	4.09	3.26	3.9	0.95	0.84	0.80	0.19	0.83	10.63	-3.40	15.95	2.22	0.45
81	4.74	3.53	4.54	0.96	0.78	0.74	0.2	1.21	12.46	-4.49	21.52	1.93	0.33
82	5.05	4.28	4.77	0.94	0.90	0.85	0.28	0.77	18.32	-1.61	24.09	2.53	0.39
83	3.57	3.29	3.36	0.94	0.98	0.92	0.21	0.28	10.82	2.71	12.00	3.01	0.34
84	4.95	3.67	4.29	0.87	0.86	0.74	0.66	1.28	13.47	0.21	21.24	2.11	0.42
85	3.43	3.04	3.18	0.93	0.96	0.89	0.25	0.39	9.24	1.59	10.91	2.82	0.37
86	4.01	3.37	3.49	0.87	0.97	0.84	0.52	0.64	11.36	3.72	13.99	2.71	0.44
87	3.05	2.38	2.81	0.92	0.85	0.78	0.24	0.67	5.66	-1.82	8.57	2.20	0.35
88	4.51	4.26	4.13	0.92	1.03	0.94	0.38	0.25	18.15	10.80	18.63	3.25	0.41
89	3.81	3.52	3.72	0.98	0.95	0.92	0.09	0.29	12.39	-2.05	14.17	2.91	0.38

Table 5 (cont): Summary of Data from pebble morphometric analysis and calculations for Ibusa Pebbles

90	3.28	3	3.17	0.97	0.95	0.91	0.11	0.28	9.00	-1.17	10.40	2.89	0.43
91	5.14	3.33	4.69	0.91	0.71	0.65	0.45	1.81	11.09	-3.88	24.11	1.53	0.34
92	3.98	3.75	3.88	0.97	0.97	0.94	0.1	0.23	14.06	-0.69	15.44	3.04	0.40
93	5.66	3.23	4.77	0.84	0.68	0.57	0.89	2.43	10.43	-2.34	27.00	1.29	0.37
94	3.91	2.86	3.57	0.91	0.80	0.73	0.34	1.05	8.18	-2.41	13.96	1.95	0.43
95	3.64	2.92	3.4	0.93	0.86	0.80	0.24	0.72	8.53	-2.08	12.38	2.30	0.36
96	4.12	2.79	3.91	0.95	0.71	0.68	0.21	1.33	7.78	-5.05	16.11	1.61	0.42
97	3.26	2.23	2.99	0.92	0.75	0.68	0.27	1.03	4.97	-3.48	9.75	1.70	0.39
98	2.93	2.5	2.71	0.92	0.92	0.85	0.22	0.43	6.25	0.14	7.94	2.62	0.44
99	3.05	2.65	2.81	0.92	0.94	0.87	0.24	0.4	7.02	1.15	8.57	2.73	0.33
100	4.69	3.4	4.44	0.95	0.77	0.72	0.25	1.29	11.56	-4.22	20.82	1.85	0.39
101	4.24	2.6	3.2	0.75	0.81	0.61	1.04	1.64	6.76	2.19	13.57	1.66	0.38
102	3.32	3.16	3.2	0.96	0.99	0.95	0.12	0.16	9.99	2.63	10.62	3.13	0.44
103	3.83	3.34	3.72	0.97	0.90	0.87	0.11	0.49	11.16	-3.16	14.25	2.61	0.35
104	3.48	2.31	3.35	0.96	0.69	0.66	0.13	1.17	5.34	-5.86	11.66	1.53	0.40
105	4.04	2.94	3.71	0.92	0.79	0.73	0.33	1.1	8.64	-2.75	14.99	1.92	0.36
106	2.83	2.26	2.42	0.86	0.93	0.80	0.41	0.57	5.11	2.75	6.85	2.49	0.43
107	4.79	2.91	4.13	0.86	0.70	0.61	0.66	1.88	8.47	-2.45	19.78	1.43	0.34
108	2.92	2.55	2.87	0.98	0.89	0.87	0.05	0.37	6.50	-4.18	8.38	2.59	0.40
109	3.67	2.49	3.52	0.96	0.71	0.68	0.15	1.18	6.20	-5.50	12.92	1.60	0.37
110	5.38	3.58	4.49	0.83	0.80	0.67	0.89	1.8	12.82	-0.08	24.16	1.77	0.43
111	3.6	2.45	3.34	0.93	0.73	0.68	0.26	1.15	6.00	-4.02	12.02	1.66	0.33
112	3.79	2.82	3.43	0.91	0.82	0.74	0.36	0.97	7.95	-1.73	13.00	2.04	0.39
113	3.38	2.79	3.31	0.98	0.84	0.83	0.07	0.59	7.78	-4.62	11.19	2.32	0.35
114	3.44	2.72	3.18	0.92	0.86	0.79	0.26	0.72	7.40	-1.76	10.94	2.25	0.42
115	5.71	3.39	5.02	0.88	0.68	0.59	0.69	2.32	11.49	-3.41	28.66	1.34	0.38
116	3.64	2.52	3.14	0.86	0.80	0.69	0.5	1.12	6.35	-0.77	11.43	1.85	0.45
117	3.82	3	3.41	0.89	0.88	0.79	0.41	0.82	9.00	0.00	13.03	2.30	0.32
118	4.55	2.2	3.41	0.75	0.65	0.48	1.14	2.35	4.84	-0.31	15.52	1.04	0.39
119	3.84	3	3.44	0.90	0.87	0.78	0.4	0.84	9.00	-0.30	13.21	2.27	0.36
120	3.43	2.64	3	0.87	0.88	0.77	0.43	0.79	6.97	0.58	10.29	2.26	0.42
121	4.88	3.87	4.34	0.89	0.89	0.79	0.54	1.01	14.98	0.44	21.18	2.36	0.35
122	4.36	3.34	3.94	0.90	0.85	0.77	0.42	1.02	11.16	-1.15	17.18	2.16	0.41
123	4.78	4.09	4.49	0.94	0.91	0.86	0.29	0.69	16.73	-0.93	21.46	2.60	0.38
124	2.8	2.46	2.6	0.93	0.95	0.88	0.2	0.34	6.05	1.00	7.28	2.77	0.44
125	3.56	2.57	3.1	0.87	0.83	0.72	0.46	0.99	6.60	-0.49	11.04	1.99	0.33
126	4.01	3.03	3.56	0.89	0.85	0.76	0.45	0.98	9.18	-0.54	14.28	2.14	0.39
127	3.64	3.39	3.56	0.98	0.95	0.93	0.08	0.25	11.49	-1.93	12.96	2.96	0.38
128	3.39	2.66	3.12	0.92	0.85	0.78	0.27	0.73	7.08	-1.66	10.58	2.23	0.44
129	3.32	2.25	3.02	0.91	0.75	0.68	0.3	1.07	5.06	-3.24	10.03	1.68	0.34
130	3.95	3.47	3.59	0.91	0.97	0.88	0.36	0.48	12.04	2.85	14.18	2.83	0.40

Table 5 (cont): Summary of Data from pebble morphometric analysis and calculations for Ibusa Pebbles

131	3.6	2.69	3.28	0.91	0.82	0.75	0.32	0.91	7.24	-1.99	11.81	2.04	0.37
132	2.65	2.49	2.54	0.96	0.98	0.94	0.11	0.16	6.20	2.00	6.73	3.07	0.43
133	2.66	1.78	2.37	0.89	0.75	0.67	0.29	0.88	3.17	-2.55	6.30	1.68	0.35
134	3.19	2.8	2.91	0.91	0.96	0.88	0.28	0.39	7.84	2.48	9.28	2.82	0.41
135	2.94	2.83	2.95	1.00	0.96	0.96	-0	0.11	8.01	-6.14	8.67	3.08	0.38
136	3.18	2.44	3.09	0.97	0.79	0.77	0.09	0.74	5.95	-4.93	9.83	2.02	0.45
137	3.32	3.15	3.25	0.98	0.97	0.95	0.07	0.17	9.92	-0.93	10.79	3.07	0.32
138	3.61	3.15	3.33	0.92	0.95	0.87	0.28	0.46	9.92	1.25	12.02	2.75	0.39
139	3.99	3.37	3.91	0.98	0.86	0.84	0.08	0.62	11.36	-4.39	15.60	2.43	0.35
140	3.04	2.41	2.86	0.94	0.84	0.79	0.18	0.63	5.81	-2.70	8.69	2.23	0.42
141	2.49	2.1	2.22	0.89	0.95	0.84	0.27	0.39	4.41	2.28	5.53	2.66	0.37
142	2.87	2.15	2.61	0.91	0.82	0.75	0.26	0.72	4.62	-1.85	7.49	2.06	0.43
143	2.3	2.09	2.55	1.11	0.82	0.91	-0.3	0.21	4.37	-18.60	5.87	2.48	0.34
144	3.48	3	3.35	0.96	0.90	0.86	0.13	0.48	9.00	-2.66	11.66	2.57	0.40
145	3.07	2.69	2.93	0.95	0.92	0.88	0.14	0.38	7.24	-1.50	9.00	2.68	0.36
146	3.43	2.79	3.27	0.95	0.85	0.81	0.16	0.64	7.78	-3.07	11.22	2.31	0.42
147	4.28	3.67	4.06	0.95	0.90	0.86	0.22	0.61	13.47	-1.63	17.38	2.58	0.35
148	4.14	3.74	3.91	0.94	0.96	0.90	0.23	0.4	13.99	0.83	16.19	2.88	0.41
149	3.97	3.03	3.53	0.89	0.86	0.76	0.44	0.94	9.18	-0.42	14.01	2.18	0.39
150	2.77	2.44	2.55	0.92	0.96	0.88	0.22	0.33	5.95	1.89	7.06	2.81	0.45
151	2.89	1.98	2.51	0.87	0.79	0.69	0.38	0.91	3.92	-1.20	7.25	1.80	0.32
152	2.7	2.45	2.68	0.99	0.91	0.91	0.02	0.25	6.00	-4.63	7.24	2.77	0.40
153	3.76	3.43	3.38	0.90	1.01	0.91	0.38	0.33	11.76	7.14	12.71	3.09	0.37
154	3.46	3.22	3.33	0.96	0.97	0.93	0.13	0.24	10.37	0.45	11.52	3.00	0.42
155	3.5	3.28	3.47	0.99	0.95	0.94	0.03	0.22	10.76	-3.88	12.15	2.95	0.35
156	2.78	2.32	2.57	0.92	0.90	0.83	0.21	0.46	5.38	-0.52	7.14	2.51	0.41
157	3.96	2.84	3.79	0.96	0.75	0.72	0.17	1.12	8.07	-4.86	15.01	1.79	0.38
158	3.19	2.85	3.14	0.98	0.91	0.89	0.05	0.34	8.12	-3.95	10.02	2.70	0.44
159	3.6	2.98	3.36	0.93	0.89	0.83	0.24	0.62	8.88	-1.36	12.10	2.45	0.33
160	3.79	3.17	3.57	0.94	0.89	0.84	0.22	0.62	10.05	-1.74	13.53	2.48	0.39
161	3	2.75	2.91	0.97	0.95	0.92	0.09	0.25	7.56	-1.53	8.73	2.89	0.37
162	4.09	2.49	3.31	0.81	0.75	0.61	0.78	1.6	6.20	-0.21	13.54	1.53	0.43
163	3.53	2.81	3.34	0.95	0.84	0.80	0.19	0.72	7.90	-2.97	11.79	2.23	0.34
164	3.32	2.46	3.05	0.92	0.81	0.74	0.27	0.86	6.05	-2.51	10.13	1.99	0.40
165	3.98	2.55	3.74	0.94	0.68	0.64	0.24	1.43	6.50	-5.18	14.89	1.46	0.38
166	3.41	2.97	3.26	0.96	0.91	0.87	0.15	0.44	8.82	-1.83	11.12	2.64	0.42
167	3.38	2.92	3.07	0.91	0.95	0.86	0.31	0.46	8.53	2.01	10.38	2.74	0.35
168	3.15	2.82	2.7	0.86	1.04	0.90	0.45	0.33	7.95	9.65	8.51	3.12	0.41
169	2.6	1.85	2.36	0.91	0.78	0.71	0.24	0.75	3.42	-2.53	6.14	1.86	0.39
170	2.93	1.98	2.63	0.90	0.75	0.68	0.3	0.95	3.92	-2.73	7.71	1.70	0.44
171	3.09	1.84	2.8	0.91	0.66	0.60	0.29	1.25	3.39	-4.50	8.65	1.30	0.33

Table 5 (cont): Summary of Data from pebble morphometric analysis and calculations for Ibusa Pebbles													
172	2.85	2.13	2.51	0.88	0.85	0.75	0.34	0.72	4.54	-0.37	7.15	2.11	0.39
173	2.95	2.42	2.79	0.95	0.87	0.82	0.16	0.53	5.86	-2.42	8.23	2.37	0.36
174	3.09	2.15	2.63	0.85	0.82	0.70	0.46	0.94	4.62	-0.15	8.13	1.90	0.42
175	2.97	1.89	2.67	0.90	0.71	0.64	0.3	1.08	3.57	-3.49	7.93	1.50	0.37
176	2.99	2.32	2.63	0.88	0.88	0.78	0.36	0.67	5.38	0.48	7.86	2.28	0.43
177	3.24	2.21	2.71	0.84	0.82	0.68	0.53	1.03	4.88	0.21	8.78	1.85	0.35
178	2.58	1.84	2.38	0.92	0.77	0.71	0.2	0.74	3.39	-3.22	6.14	1.84	0.41
MEAN	4.02	3.00	3.51	0.91	0.86	0.78	0.50	1.02	9.70	-0.61	14.94	2.25	0.39
SD	2.15	0.85	0.95	0.09	0.10	0.12	1.96	2.02	6.01	6.02	9.67	0.56	0.04

L - Long Axis, S - Short Axis, I - Intermediate Axis, I/L - Elongation Ratio (ER), S/L - Flatness Ratio (FR), S/I - Another measure of flatness, OPI - Oblate – Prolate (OP) Index, MPSI - Maximum Projection Sphericity Index, FI - Flatness Index

Sphericity is a measure of equidimensionality i.e. the relation between the three axes of a particle or in other words how far a pebble can be considered to be a sphere. The maximum projection sphericity (MPS) suggested by Sneed and Folk (1958) was applied in the present research. The square root of the ratio of square of the short axis and the product of the long and middle axes is defined as MPS and mathematically it is expressed as (S2/LI)1/3. This is the best parameter that describes the behaviour of particles during the transport in a fluid mediation. The values of MPS of pebbles in Asaba are between 0.79 and 3.20 with mean value of 2.21 and that of Ibusa are between 0.21 and 3.29 with mean value of 2.25 (Figures 4a and 4b).

Form is a quantification of the bond in the three mutually perpendicular dimensions of a pebble. It is applied to show that particles which have the same MPS value can differ in the ratios between their axes. The form category of each batch of pebbles was determined with the help of the diagram of Sneed and Folk (1958) which is the Sphere-combinations diagram. By plotting the data in this diagram, three major forms that appeared were compact-bladed (CB), compact-platy (CP), and compact (C) that accounted 55, 39.1, and 6 percent respectively of Asaba and 51, 46 and 3 percent of Ibusa respectively.

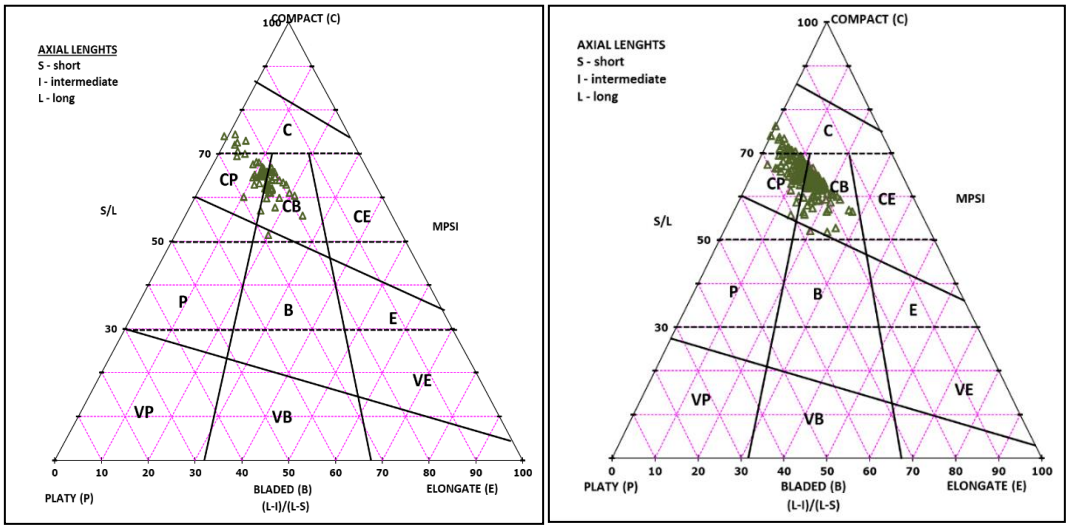

Figure 4a: Sphericity-form classification of Asaba pebbles plotted on Sneed and Folk's (1958) diagram, showing dominant compact-bladed (CB) and compact-platy (CP) forms (adapted from Nfor, 2009).

Figure 4b: Sphericity-form classification of Ibusa pebbles plotted on Sneed and Folk's (1958) diagram, showing dominant compact-bladed (CB) and compact-platy (CP) forms (adapted from Nfor, 2009).

KEY - Compact Elongate (CE), Elongate (E), Compact (C), Compact Bladed (CB), Compact Prolate (CP), Prolate (P), Very Elongate (VE), Very Bladed (VB) and Bladed (B)

Roundness is a parameter of curvature of corners and sides of a particle. Measuring of roundness was done using the roundness measuring process, the obtained mean roundness was 36 percent in Asaba pebbles and 38 percent in Ibusa pebbles (Wadell, 1932). Most of the pebbles in the research location fall under the subrounded category. Flatness is short axis divided by the long axis i.e. S/L (Sames, 1966; Lutig, 1962). The meanings of the ratios of flatness of the pebbles indicate that the ratio of the pebbles in Asaba is 0.77 and in Ibusa, it is 0.78.

The ratio of intermediate to long axis is known as elongation, i.e., I/L (Lutig, 1962; Sames, 1966). The values of elongation of pebbles in the study area vary between 0.68 and 1.00 with the mean of 0.91 in Asaba and 0.70 to 1.11 with the mean of 0.91 in Ibusa. The Oblate-Prolate Index (OPI) is used to determine the proximity of the intermediate axis to long axis or short axis. It is mathematically computed as: OPI = [(L - I)/ (L - S) - 0.5)/ SL] (Dobkins and Folk, 1970). Computed OPI values vary between -6.37 to 5.00 with a mean of -1.10 of Asaba pebbles and -18.60 to 65.10 with a mean of -0.61 of Ibusa pebbles. The high number of negative OPI values indicates that the disc pebbles are common in the study area.

Lack of metamorphic foliation and micaceous inclusions and only monomineralic quartz indicate that the quartzose pebbles are the product of the parent rock vein quartz. This means that the source area that gave rise to veins of the quartz rocks was the basement rocks that were fractured because of jointing, faulting, sheeting or exfoliation. These inherited factors are therefore found to be the cause of the initial random shape and size; hence the readings of the sphericity. This is in harmony with the results of (Blatt, 1959; Smalley, 1966). These original form and shape are continuous in the sediments regardless of the wear and tear that take place as a consequence of abrassion throughout transportation and provide overriding values of sphericity and roundness (Krumbein, 1941 and Drake, 1970). As Table 4 and Table 5 are compared to the results of figures 5a and 5b it can be seen that of the eight different member forms the blade form, the discoid form, the very oblate spheroid form and the prolate-spheroid form of pebbles were totally absent.

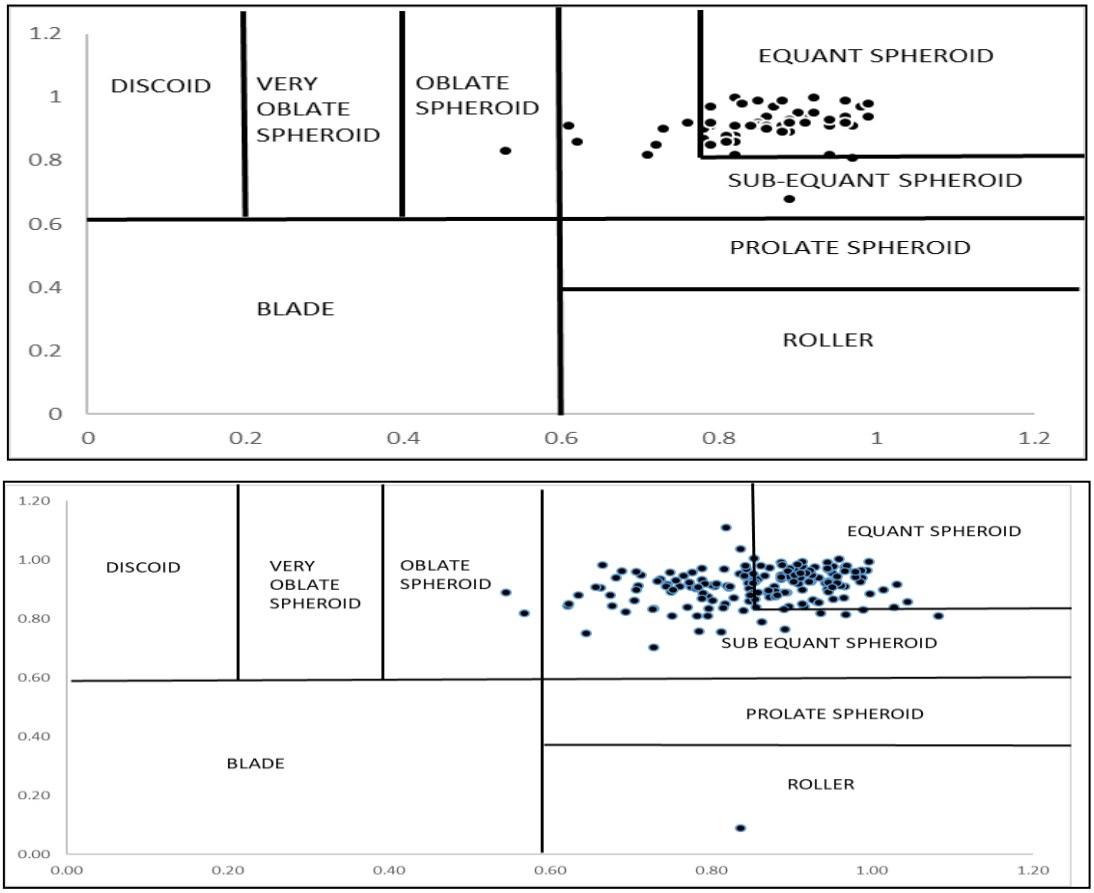

Figure 5a: Zingg (1935) form classification diagram for Asaba pebbles showing particle shape distribution.

Figure 5b: Zingg (1935) form classification diagram for Ibusa pebbles showing particle shape distribution. Samples predominantly plot as equant spheroid (ES) and sub-equant spheroid (SES) categories, with minor occurrences of discoid (D), oblate spheroid (OS), very oblate spheroid (VOS), prolate spheroid (PS), and roller (R) forms, consistent with fluvial transport conditions.

The percentage of oblate spheroid was only 2% whereas the sub-equant and equant spheroid forms made 98 and 99 percent of the pebble population respectively, in Asaba, and 1.8 percent of the pebbles at Ibusa respectively. This means that the initial shapes that were emitted in the source region were mostly sub-equant and equant spheroid (Figures 5a and 5b). The Ibusa and Asaba pebbles are generally diagnostically indicative of high-energy fluvial/beach deposition conditions involving intense abrasion, longer periods of transportation, and sorting by the hydraulic process (Okon et al., 2018).

Equant/spheroid pebbles and fluvial environments are long-term relationships, since Equant (spheroid) pebble forms are especially informative of fluvial depositional systems, since in fluvial environments, the tumbling action persistently at multidirectional bedload transport is more likely to produce equidimensional particles (Sneed and Folk 1958). This was shown in the work which showed that fluvial systems are selective in the generation and retention of spheroidal clasts due to the consistent reorientation during saltation and rolling which promotes even abrasion over all axes, high energy conditions select clasts with a high degree of sphericity through breakdown or removal by downstream transport and as a result of this lack of strong unidirectional currents (as found on a beach), selective flattening does not occur (Dobkins and Folk, 1970).

The other values of roundness were 36 percent to 38 percent (grossly subrounded), meaning fluvial environment, which is in agreement with the upper limit value, who set the roundness range values of fluvial environment between 20 percent and 70 percent (Table 6 as compiled in (Lutig, 1962; Obasi et al., 2015; Ephraim et al., 2015; Ojong, 2023 and Madukwe et al., 2025). According to this the Ibusa and Asaba values indicate a transport medial distance of the pebbles provenance.

Table 6: Roundness classification system showing: (1) Wadell index ranges, (2) corresponding descriptive classes (angular to well-rounded), and (3) environmental interpretations for each category (glacial to fluvial/beach systems) (Lutig, 1962).

Roundness Class	Wadell Roundness Index (%)	Environmental Interpretation
Very Angular	0–10%	Mostly glacial or freshly broken material
Angular	10–20%	Glacial/fluvio-glacial
Subangular	20–30%	Proximal fluvial or glaciofluvial
Subrounded	30–50%	Fluvial (dominant in many river systems)
Rounded	50–70%	Mature fluvial or beach
Well Rounded	70–100%	High-energy beach, long-distance fluvial

In addition, there were bivariate plots of roundness versus elongation ratio (Sames, 1966). The plots (figure 6a of Asaba and figure 6b of Ibusa) indicate that 92.4 percent of the Asaba samples had been deposited under fluvial environment and remainder (7.6 %) had been deposited under transitional setting and none had represented littoral environment. Likewise, 91.6 percent of the Ibusa samples had been deposited in a fluvial setting and the remainder (8. 4 %) had been deposited in a transitional setting, and none were a littoral setting. This synergetically with the indicators of palaeoenvironment applied previously in this study can also be an indication of a fluvial environment.

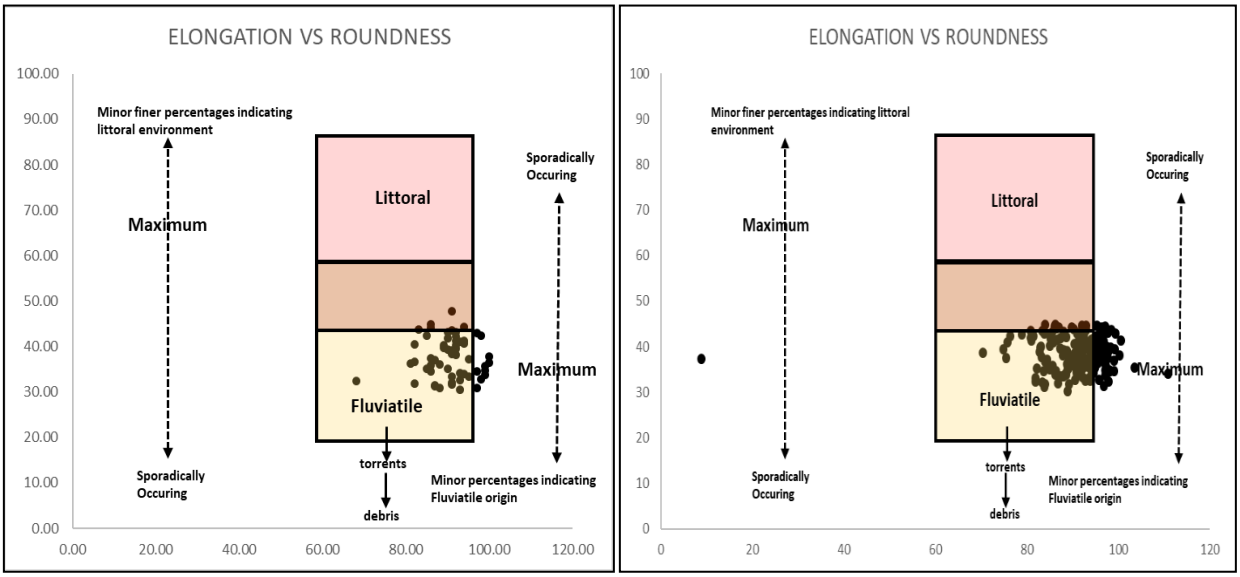

Figure 6a: Discrimination of fluvial and littoral depositional environments for Asaba pebbles using roundness versus elongation ratio.

Figure 6b: Fluvial versus littoral process discrimination chart for Ibusa pebbles, based on roundness versus elongation ratio. Data plot dominantly within the fluvial field, supporting a riverine depositional environment (modified after Sames, 1966).

Have quantitatively determined that the present river systems have 25-40% of the equant particle as compared to the beach settings at the same level of energy (Blott and Pye, 2012). This is complemented by the observations of the field as stated that argues that sphericity indices above 0.7 prevail in active channel deposits by (Bradley, 1970). Here, especially the concept of subsequent spheroid (following Krumbein 1941) which argues that fluvial systems increasingly transform inherited forms to spheroid ones can be relevant, both in the sense where it is implied that it is through an attritional process of rounding during transport and through a process of hydraulic sorting where equant shapes become concentrated in lags of the channel (Attal and Lave 2009; Garzanti, 1986).

The 0.66 line of sphericity has also been employed to identify the beach and river pebbles with the lower values (<0.66) being unique of the beach and the higher values (>0.66) being indicative of fluvial environment by (Dobkins and Folk, 1970). This indicates a predominantly fluvial environment with a 100% in Asaba and an approximation of 99.3% in Ibusa of pebble fluvial ≥0.66 and a slight percentage of the pebbles under the 0.66 line (figure 6a and 6b).

Also used the 0.66 sphericity line to discriminate beach and river pebbles, the lower values (<0.66) are typical of beach, while the higher values (>0.66) are suggestive of fluvial environment (Dobkins and Folk, 1970). With a 100% in Asaba (figure 7a) and about 99.3% in Ibusa (figure 7b) of the pebble sphericity ≥0.66, and a negligible percentage of the pebbles below the 0.66 line, a dominantly fluvial environment is suggested.

The range of OPI values (-6.37 to 5.00) with an average of -1.10 in Asaba and (-18.60 to 65.10) with an average of 0.61 in Ibusa falls within the -1.00 to +5.00 range of Dobkins and Folk (1970), suggesting a fluvial environment. Negative values indicate pebbles whose 5.5% of the pebbles were elongate, while the compact and compact-bladed forms each constitute 47.1% of the pebble population. This indicates that the original forms released from the source area were dominantly bladed and compact bladed. Compact, compact-bladed and elongate pebble forms are diagnostic of a fluvial depositional environment, for the Nsugbe pebbles (Dobkins and Folk, 1970).

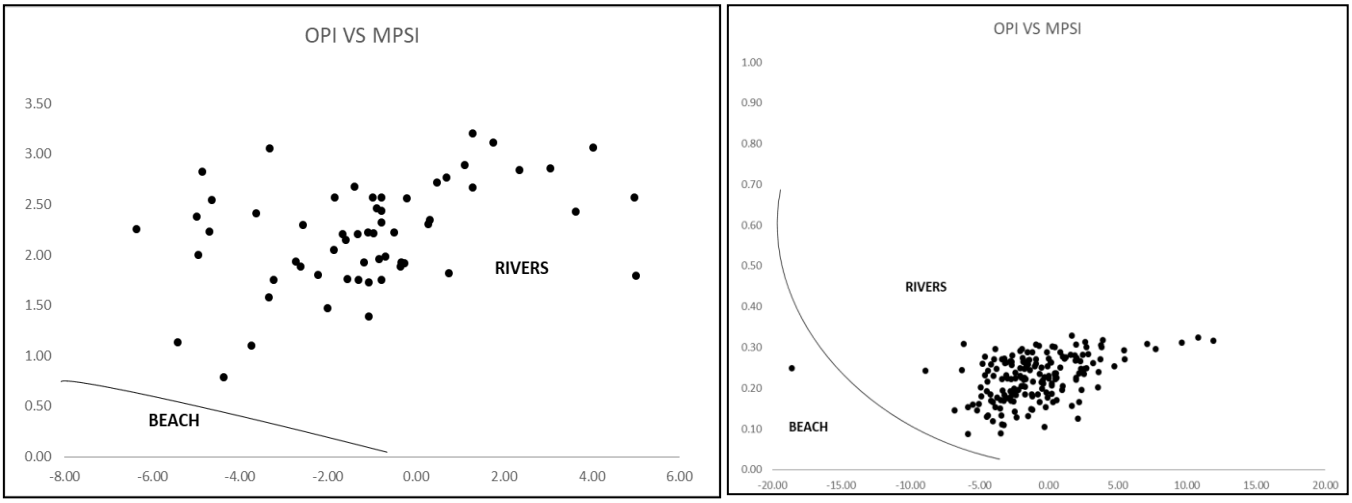

Figure 7a: Discrimination of fluvial and beach depositional environments using Maximum Projection Sphericity Index (MPSI) vs. Oblate-Prolate Index (OPI). Average values for Asaba pebbles (this study) plot within the fluvial field, consistent with thresholds defined by (Dobkins and Folk, 1970) (adapted from (Nfor, 2009).

Figure 7b: Discrimination of fluvial and beach depositional environments using Maximum Projection Sphericity Index (MPSI) vs. Oblate-Prolate Index (OPI). Average values for Ibusa pebbles (this study) plot within the fluvial field, consistent with thresholds defined by (Dobkins and Folk, 1970) (adapted from (Nfor, 2009).

4. Conclusion

This study clearly shows that the pebbly sandstones were mainly deposited in a fluvial environment. The measurements of pebble shape and size, such as roundness, flatness ratio, elongation ratio, and maximum projection sphericity index, all support this conclusion. For example, the average maximum projection sphericity index (MPSI) for the pebbles was found to be around 2.1 (Table 7), which is typical of river transport. Additionally, about 87% of the pebbles had a sphericity greater than 0.65, placing them firmly within the fluvial environment based on the bivariate plots used in this study.

Table 7: Palaeoenvironmental interpretation of pebbles Asaba and Environs based on morphometric indices: (1) roundness (36% mean), (2) sphericity (MPSI >0.65), (3) flatness/elongation ratios, and (4) Zingg form distribution, collectively indicating fluvial depositional conditions.

Morphometric Parameter	Characteristics Exhibited by the Pebbles	Environmental Indications	References
Roundness	Mean values: 36% (Asaba), 38% (Ibusa)	Fluviatile (subrounded)	Lutig (1962); Wadell (1932)
Flatness Ratio (S/L)	Mean values: 0.77 (Asaba), 0.78 (Ibusa)	Fluviatile (moderate flatness)	Lutig (1962); Sames (1966)
Elongation Ratio (I/L)	Mean values: 0.91 (both locations)	Fluviatile (near-equidimensional)	Lutig (1962); Sames (1966)
Maximum Projection Sphericity (MPSI)	Mean values: 2.21 (Asaba), 2.25 (Ibusa)	Fluviatile (MPSI > 0.66)	Dobkins and Folk (1970)
Oblate-Prolate Index (OPI)	Mean values: -1.10 (Asaba), -0.61 (Ibusa)	Fluviatile (negative OPI dominance)	Dobkins and Folk (1970)
Pebble Form (Zingg Classification)	Dominant forms: Compact (C) and Compact-Bladed (CB)	Fluviatile (equant to bladed)	Sneed and Folk (1958)
Bivariate Plots (MPSI vs. OPI)	92.4% fluvial (Asaba), 91.6% fluvial (Ibusa)	Dominantly fluvial	Dobkins and Folk (1970)

These findings suggest that the sediments came from a high-energy river system, likely originating from nearby highlands. The slightly higher sphericity observed at Ibusa compared to Asaba suggests that the river flow likely originated from the Asaba area and moved toward Ibusa, indicating a flow direction from Asaba to Ibusa. The negligible percentage of beach-like pebbles also indicates that coastal or shoreline processes played a little to no role in the deposit formation. Overall, the combination of morphometric data and sedimentological evidence confirms that the dominant depositional environment during the time of sedimentation was fluvial.

This study therefore helps to better understand the palaeoenvironment and sediment transport history of the area, providing a clearer picture of the basin's geological evolution during the Oligocene-Miocene period.

References

Adeoye, J. A., Jolayemi, V. O., and Akande, S. O., 2022. Sedimentology and foraminiferal paleoecology of the exposed Oligocene–Miocene Ogwashi-Asaba Formation in Issele-Uku area, Anambra Basin, southern Nigeria: A palaeoenvironmental reconstruction. Journal of Palaeogeography, 11(4), Pp. 618-628.

Adojoh, O. C., Marret, F., Duller, R., Osterloff, P. L., Oboh-Ikuenobe, F. E., and Saylor, B. Z., 2023. Stages of palaeoenvironmental evolution, climate and sea level change of the Niger Delta, east Equatorial Atlantic: Novelty from elemental tracers, sedimentary facies and pollen records. The Holocene, 33(7), Pp. 781-790.

Adojoh, O., Marret-Davis, F., Osterloff, P., Hart, M., Ikuenobe, F., Weakley, H., and Agbogun, H., 2025. Sedimentation rates, coastal delta accretion, and stratigraphic datum of the Late Pleistocene–Mid-Holocene transition in the East Equatorial Atlantic: New concept from calcareous nannoplankton. The Holocene, 35(4), Pp. 409-419.

Ajidahun, J., Oluwajana, O. A., Ifanegan, A. S., and Odusanwo, Y. O., 2025. Structural and petrophysical assessment of CO2 storage in depleted Z-field reservoirs, Offshore Niger Delta Basin. Marine Georesources and Geotechnology, Pp. 1-18.

Akpere E. and Asadu, A. N., 2025. Sedimentary Facies and Grain Size Distribution; Insights into Ogwashi-Asaba Formation, Niger Delta Basin. FUPRE Journal of Scientific and Industrial Research, 2579-1184, 2025, Vol 9, Issue 1, p380

Alamu, K. O., 2023. Structural Characterisation of Alamu Field, Niger-Delta. Unpublished B.Sc. Project, Kwara State University, Malete, Nigeria. September 2023.

Allen, C. A., Udo, I. G., Harry, T. A., and Ekot, A. E., 2024. Granulometric and pebble morphometric analyses of sandstone Lithofacies of the Ameki formation in northeastern part of Akwa Ibom State, Niger Delta, Nigeria. Researchers Journal of Science and Technology, 4(1), Pp. 32-44.

Amasi, A., Wynants, M., Blake, W., and Mtei, K., 2021. Drivers, impacts and mitigation of increased sedimentation in the hydropower reservoirs of East Africa. Land, 10(6), 638.

Anyanwu, I. E., Okeugo, C. G., and Orji, I. K., 2021. Granulometric and Pebble Morphometric Analyses of Rock Units Within the Uzuakoli-Ahaba Axis and Environs: An Outcome of Geological Mapping and Outcrop Studies. Petroleum and Coal, 63(3).

Anyiam, O. A., Hoggmascall, N., and Amogu, D. K., 2021. Basin margin sediment wedge build out of the Eastern Niger Delta: application of shelf-edge trajectory pattern studies. Journal of Petroleum Exploration and Production, 11(3), Pp. 1093-1100.

Aransiola, S. A., Zobeashia, S. L. T., Ikhumetse, A. A., Musa, O. I., Abioye, O. P., Ijah, U. J. J., and Maddela, N. R., 2024. Niger Delta mangrove ecosystem: Biodiversity, past and present pollution, threat and mitigation. Regional Studies in Marine Science, 103568.

Attal, M., and Lavé, J., 2009. Pebble abrasion during fluvial transport: Experimental results and implications for the evolution of the sediment load along rivers. Journal of Geophysical Research: Earth Surface, 114(F4).

Blott, S. J., and Pye, K., 2012. Particle size scales and classification of sediment types based on particle size distributions: Review and recommended procedures. Sedimentology, 59(7), Pp. 2071-2096.

Bluck, B. J., 1967. Sedimentation of beach gravels: examples from South Wales. Journal of Sedimentary Research, 37(1), Pp. 128-156.

Boggs, S., 2006. Principles of sedimentology and stratigraphy: Pearson Prentice Hall. Upper Saddle River, New Jersey, 581.

Bradley, W. C., 1970. Effect of weathering on abrasion of granitic gravel, Colorado River (Texas). Geological Society of America Bulletin, 81(1), Pp. 61-80.

Chima, K. I., Granjeon, D., Do Couto, D., Leroux, E., Gorini, C., Rabineau, M., ... and Glukstad, M. M., 2022. Tectono-stratigraphic evolution of the offshore western Niger Delta from the Cretaceous to present: Implications of delta dynamics and paleo-topography on gravity-driven deformation. Basin Research, 34(1), Pp. 25-49.

Chima, K. I., Granjeon, D., Do Couto, D., Leroux, E., Gorini, C., Rabineau, M., ... and Glukstad, M. M., 2022. Tectono-stratigraphic evolution of the offshore western Niger Delta from the Cretaceous to present: Implications of delta dynamics and paleo-topography on gravity-driven deformation. Basin Research, 34(1), Pp. 25-49.

Dobkins, J. E., and Folk, R. L., 1970. Shape development on Tahiti-nui. Journal of Sedimentary Research, 40(4), Pp. 1167-1203.

Dobkins, J. E., and Folk, R. L., 1970. Shape development on Tahiti-nui. Journal of Sedimentary Research, 40(4), Pp. 1167-1203.

Ejeh, O. I., 2021. Geochemistry of rocks (Late Cretaceous) in the Anambra Basin, SE Nigeria: insights into provenance, tectonic setting, and other palaeo-conditions. Heliyon, 7(10).

Enuenwosu, C. U., Ohwo, M. U., and Ehinlaiye, A. O., 2024. Sedimentary

Petrology and Palaeogeography of the Eocene-Sandstone Facies of Ilaro Formation, Dahomey Basin, South-Western Nigeria. International Journal of Earth Sciences Knowledge and Applications, 6(3), Pp. 357-373.

Ephraim, B. E., Amaechina, C., and Odumodu, C. F., 2015. Pebble morphometric investigations on pebbles belonging to the Benin formation at NSIE and environs, Southeastern Nigeria. Pelagic Research Library, 28, Pp. 49-55.

Eze, O. E., Okiwelu, A. A., Ekwok, S. E., Abdelrahman, K., Alzahrani, H., Ben, U. C., and Eldosouky, A. M., 2024. Delineation of deep-seated crustal structures from magnetic data in the southeastern part of the Niger Delta basin, Nigeria. Frontiers in Earth Science, 12, 1439199.

Fagbemi, O. I., Olayinka, A. I., Oladunjoye, M. A., and Edigbue, P. I., 2024. Focused reservoir characterisation: analysis of selected sand units using well log and 3-D seismic data in'Kukih'field, Onshore Niger Delta, Nigeria. Scientific Reports, 14(1), Pp. 13763.

Flemming, B. W., 2007. The influence of grain-size analysis methods and sediment mixing on curve shapes and textural parameters: implications for sediment trend analysis. Sedimentary Geology, 202(3), Pp. 425-435.

Ideozu, R. U., and Ikoro, D. O., 2015. Sedimentology of Conglomeratic Beds within Odoro Ikpe–Arochukwu Axis: Afikpo Basin, Southeastern Nigeria. Int J Min Geol, 5(2), Pp. 1-15.

Ideozu, R. U., Mba-Otike, M. N. and Odumoso, S., 2025. Integrated Characterization and Forecasting of Overpressure Mechanisms in the 'Nge' Field, Offshore Niger Delta: Insights from Rock Properties – Seismic Velocity Cross-Plot Analysis. International Journal of Research and Scientific Innovation. XII. 532-546. 10.51244/IJRSI.2025.12010048.

Ideozu, R. U., Mba-Otike, M. N., and Odiaka, N. I., 2025. Reservoir Properties and Compactmentalisation of Odiemelu Field Onshore Niger Delta, Nigeria. Scientia Africana, 24(6), Pp. 1-10.

Illenberger, W. K., 1991. Pebble shape (and size!). Journal of Sedimentary Research, 61(5), Pp. 756-767.

Jolayemi, V. O., Adeoye, J. A., and Akande, S. O., 2023. Hydrocarbon potential of shales and lignites of Oligocene-Miocene Ogwashi-Asaba formation exposed in Issele-Uku of Anambra Basin, Southern Nigeria, as both conventional and unconventional resources. Energy Exploration and Exploitation, 41(2), Pp. 518-533.

Kanhaiya, S., Singh, B. P., Tripathi, M., Sahu, S., and Tiwari, V., 2017. Lithofacies and particle-size characteristics of late Quaternary floodplain deposits along the middle reaches of the Ganga River, central Ganga plain, India. Geomorphology, 284, Pp. 220-228.

Kasim, S. A., Ismail, M. S., and Ahmed, N., 2023. Grain size statistics and morphometric analysis of Kluang-Niyor, Layang-Layang, and Kampung Durian Chondong tertiary sediments, onshore peninsular Malaysia: implications for paleoenvironment and depositional processes. Journal of King Saud University-Science, 35(2), 102481.

Lawson, I. T., Honorio Coronado, E. N., Andueza, L., Cole, L., Dargie, G. C., Davies, A. L., Laurie, N., Okafor-Yarwood, I., Roucoux, K. H. and Simpson, M., 2022. The vulnerability of tropical peatlands to oil and gas exploration and extraction. Progress in Environmental Geography, 1(1-4), Pp. 84-114.

Lutig, G., 1962. The shapes of pebbles in continental, fluviatile and marine facies. International Association of Geology and Geophysics. International Association of Hydrogeologists. 59: Pp. 253-258.

Madi, K., and Ndlazi, N. Z., 2020. Pebble morphometric analysis as signatures of the fluvial depositional environment of the Katberg Formation near Kwerela River around East London, Eastern Cape Province, South Africa. Arabian journal of geosciences, 13(5), Pp. 235.

Madukwe, H. Y., Aturamu, A. O., and Ilori, A. O., 2025. Morphometry and Paleoenvironment of Pebbles from the Agbani Sandstone, southeast Nigeria. Jordan Journal of Earth and Environmental Sciences, 16(1).

Madukwe, H. Y., Aturamu, A. O., and Ilori, A. O., 2025. Morphometry and Paleoenvironment of Pebbles from the Agbani Sandstone, Southeast Nigeria. Jordan Journal of Earth and Environmental Sciences, 16(1).

Mba-Otike, M. N., Ideozu, R. U. and Odiaka, N. I., 2025. Petrophysical Evaluation of Nwosa Field, Offshore Niger Delta, Nigeria; Implication for Depositional Environment. International Journal of Research and Scientific Innovation. XII. Pp. 876-883. 10.51244/IJRSI.2025.12010076.

Mba-Otike, M. N., Ideozu, R. U., and Odiaka, N. I., 2025. Petrophysical Evaluation of Nwosa Field, Offshore Niger Delta, Nigeria; Implication for Depositional Environment. International Journal of Research and Scientific Innovation, 12, 876-883.

Ndjigui, P. D., Bessa, A. Z. E., Priso, E. N. E., and Sababa, E., 2023. Critical evaluation of weathering indexes for paleoclimatic reconstructions: indication from recent sediments and Mesozoic sedimentary rocks from equatorial to tropical Central Africa (Cameroon and Nigeria). Arabian Journal of Geosciences, 16(7), 415.

Nfor, B. N., 2009. Palaeodepositional environmental diagnosis of the Nsugbe area and environs, Anambra state, southeastern Nigeria: an application of pebble Morphometric studies. Global Journal of Geological Sciences, 7(2).

Obasi, P. N., Okoro, A. U., Igwe, E. O., and Edene, E. N., 2015. Petrological characteristics and paleo-depositional environment of the sandstones of the ameki group (eocene) in Bende and Isimkpu Areas, Southeastern Nigeria. Journal of Applied Geology and Geophysics (IOSR-JAGG), 3(5), Pp. 09-15.

Odesa, G. E., Ozulu, G. U., Eyankware, M. O., Mba-Otike, M. N., and Okudibie, E. J., 2024. A holistic review of three-decade oil spillage across the Niger Delta Region, with emphasis on Its impact on soil and water. World Sci. News, 190, Pp. 119-139.

Odudukurudu, T. L., and Samuel, V. C., 2023. Lithofacies and Depositional Environment of the Outcropping Sediments of the Ogwashi-Asaba Formation, Niger Delta Basin. International Journal of Science Inventions Today. IJSIT, ISSN 2319-5436, 2023, 12(3), Pp. 180-197.

Ogbe, O. B., Osokpor, J., Emelue, C. V., and Ocheli, A., 2023. Morphometric analysis of pebbles in verification of transport processes and interpretation of palaeoenvironment: A case study from the Ogwashi Formation (Oligocene), Niger Delta Basin, Nigeria. Geologos, 29(1), Pp. 21-31.

Ojenabor, F., Fadiya, S. L., and Adepehin, E. J., 2024. Paleocene–Late Oligocene dinoflagellate cysts biostratigraphy, onshore Niger Delta. Geosystems and Geoenvironment, 3(3), 100280.

Ojong, R. A., Ugar, S. I., Odong, P. O., Emeka, C. N., and Itowe, K., 2023. Pebble morphometry and sieve analysis: tools in determining the depositional environments of sediments in oron and environs. Global Journal of Geological Sciences, 21(2), Pp. 201-213.

Ojong, R. A., Ugar, S. I., Odong, P. O., Emeka, C. N., and Itowe, K., 2023. Pebble morphometry and sieve analysis: tools in determining the depositional environments of sediments in Oron and environs. Global Journal of Geological Sciences, 21(2), Pp. 201-213.

Okon, E. E. and Ojong, R. A., 2019. Palaeoenvironmental Analysis and Its Significance in Sedimentology: Case Study of the Conglomerate Facies of the Awi Formation. In book: Advances and Trends in Physical Science Research Vol. 2 (pp.84 - 98). Publisher: Book Publisher International

Okon, E. E., and Ojong, R. A., 2019. Palaeoenvironmental analysis and its significance in sedimentology: case study of the conglomerate facies of the Awi Formation, Calabar Flank, Southeast Nigeria. Advances and trends in physical science research, 2.

Okon, E. E., Asi, M. O., and Ojong, R. A., 2018. Morphometric studies of pebbles from Ewen area, Calabar flank, southeastern Nigeria: implications for Palaeoenvironmental reconstruction. Physical Science International Journal, 17(4), Pp. 1-12.

Okon, E. E., Asi, M. O., and Ojong, R. A., 2018. Morphometric studies of pebbles from Ewen area, Calabar flank, southeastern Nigeria: implications for Palaeoenvironmental reconstruction. Physical Science International Journal, 17(4), Pp. 1-12.

Okoro, A.U., Onuigbo, E.N., Akpunonu, E.O. and Obiadi, I. I., 2012. Lithofacies and pebble morphogenesis: keys to Palaeoenvironmental interpretation of the Nkporo formation, Afikpo Sub-Basin, Nigeria. J Environ Earth Sci 2(6):2012

Omo-Irabor, O. O., Ogala, J. E., Abiodun Etobro, I. A., Ejeh, O. I., and Eziashi, C. F., 2024. Geometry and depositional environment of the sandy aquifers in the Oligocene-Miocene Ogwashi-Asaba Formation, southern Nigeria. Petroleum and Coal, 66(4).

Omoruyı, D. I., Ilevbare, M., Ehinlaıye, A. O., and Akujıeze, C. N., 2022. Geochemical Discriminant for Provenance Characterisation of Some Clay Deposits in Edo State, Nigeria. International Journal of Earth Sciences Knowledge and Applications, 4(3), Pp. 407-418.

Omosanya, K. O., and Alves, T. M., 2013, June. Provenance of a Blocky Debris Flow Deposit in Mid-Continental Slopes (Espírito Santo Basin, SE Brazil). In 75th EAGE Conference and Exhibition incorporating SPE EUROPEC 2013 (pp. cp-348). European Association of Geoscientists and Engineers.

Oyebanjo, O., Ekosse, G. I., and Odiyo, J., 2021. U–Pb ages of detrital zircons in Cretaceous–Paleogene/Neogene kaolins within Eastern Dahomey and Niger Delta Basins (Nigeria) as provenance indicators. Scientific Reports, 11(1), 13861.

Pissart, A., Duchesne, F., and Vanbrabant, C., 1998. La détermination pratique des intervalles de confiance des comptages de cailloux et des mesures d'emousse; comparaison des mesures d'emousse de Cailleux et de Krumbein. Géomorphologie: relief, processus, environnement, 4(3).

Salim, M. A. A., 2021. Determination of reservoir characteristics of Abu Gabra Formation by using well logging methods, Neem-k area, a Muglad Basin, Sudan (Doctoral dissertation, Al-Neelain University).

Samal, P., Subramanian, S. R., Srivastava, J., Kawsar, M., Manoj, M. C., Gurumurthy, G. P., and Bhushan, R., 2023. A 2600-yr multiproxy record for climate and vegetation reconstruction along the Mahanadi River delta, east coast of India. The Holocene, 33(7), Pp. 860-879.

Sames, C. W., 1966. Morphometric data of some recent pebble associations and their application to ancient deposits. Journal of Sedimentary Petrology 36: Pp. 126-142.

Sneed, E. D., and Folk, R. L., 1958. Pebbles in the lower Colorado River, Texas: a study in particle morphogenesis. The Journal of Geology, 66(2), Pp. 114-150.

Stratten, T., 1974. Notes on the application of shape parameters to differentiate between beach and river deposits in southern Africa. South African Journal of Geology, 77(3), Pp. 383-384.

Sun, L. X., Chen, X. G., Wu, D. D., Liu, L. H., Jin, G. R., and Wei, X. Q., 2022). Provenance of sediments from the Niger Delta, Gulf of Guinea: Evidence from geochemistry. Journal of Marine Systems, 235, 103794.

Tijani, M. N., 2023. Geology of Nigeria. In Landscapes and landforms of Nigeria (pp. 3-32). Cham: Springer Nature Switzerland.

Udo, I. G., Udofia, P. A., Etukudo, N. J., and Adesina, D. A., 2023. Palaeoenvironmental interpretation of the exposed section of the Benin Formation in the southeastern part of the Niger Delta Basin, Nigeria: A pebble morphometric approach. IOSR Journal of Applied Geology and Geophysics, 11, Pp. 12-19.

Wadell, H., 1932. Volume, shape, and roundness of rock particles. The Journal of Geology, 40(5), Pp. 443-451.

Wali, S. U., Dankani, I. M., Abubakar, S. D., Gada, M. A., and Umar, K. J., 2021. Detailed Hydrogeological and Hydro Chemical Reassessment of the Niger Delta Basin, South-South Nigeria. J. Energy Eng. Thermodyn. (JEET), 1(01), Pp. 6-41.

Yuan, S. Q., Pan, C. F., Qin, Y. Q., He, Z. J., Jiang, H., Liu, X. B., Liu, J.G. and Ou, Y. F., 2025. Stratigraphic Development and Paleogeographic Evolution Characteristics of Sedimentary Basins in the East Africa Region. In the International Field Exploration and Development Conference (pp. 355-375). Springer, Singapore.

Zhang, J. J., Wu, S. H., Hu, G. Y., Yue, D. L., Chen, C., Chen, M., and Wang, L. Q., 2023. Sedimentary–tectonic interaction on the growth sequence architecture within the intraslope basins of deep-water Niger Delta Basin. Journal of Palaeogeography, 12(1), Pp. 107-128.

Cite the Article: Mba-Otike, Michael Nelson, Okengwu, Kingsley Onyekwere and Ideozu, Richmond Uwanemesor (2026). Pebble Morphometric Analysis of Oligocene-Miocene Deposits in Asaba and Environs, Delta State, Southern Nigeria: Implications for Palaeoenvironment and Palaeodeposition. Malaysian Journal of Geosciences, 10(2): 64-79.